Development of Algorithm for Assessment of Cloud Properties

Tanutdech Rotjana Kusol

Abstract— The aim of this study is to development of algorithm for assessment of cloud properties in the atmosphere using satellite data. The work began by analyzing cloud cover in Thailand. To reduce possible confusion between high clouds and precipitation-causing clouds, the high clouds were removed using the spectral method based on the a priori knowledge-based threshold. This study successful development of algorithm for assessment of cloud properties in the atmosphere using satellite data, which will be use for early warnings of precipitation-causing clouds in Thailand.

Index Terms— Development of algorithm, satellite data, a priori knowledge-based threshold.

I. INTRODUCTION

The stability of earth's radiation determines current patterns of weather conditions and climate change, and can be studied by satellite observations of the developing allocation and the variety of cloud structures [1] – [4]. Early investigations have focused on the importance of whole cloud cover, and ignored the effect of cloud type variation [5]. The properties of cloud top particles can be obtained from multi-channel near infrared data. Using reflected emitted radiances of about 1.6 μm, 2.1 μm and 3.9 μm has proven very useful in studying the microphysical clouds properties, while being restricted to complete daylight operations [6]. The clouds aerosols precipitation tool classifies imagery using tables adapted to "day microphysical" and "night microphysical" environments [7], allowing cloud microphysical based scene classification, which is helpful for rain area explanation [8]. Conversely, the cloud top temperature to precipitation relationship is indirect, with major variations in the relationship during the lifetime of a precipitation event, between rain systems, and between climatologically regimes. However, IR-based techniques combine a degree of simplicity with readily available data [9]. They also include VIS-IR in early algorithms and methods i.e. VIS-IR [10]. Cloud top height classifications are comparisons from an advanced space-borne thermal emission and reflection radiometer (ASTER), a multi-angle imaging spectroradiometer (MISR), and a moderate-resolution imaging spectroradiometer (MODIS) [11]. Cloud detection with MODIS also improves the MODIS cloud mask for collection and the estimation of instantaneous net surface long wave radiation from MODIS cloud free data [12] – [14].

II. THE STUDY AREA

A. The study area

Thailand (see in Figure 1) is located in the tropical area between latitudes 5 o 37 ′ N to 20 o 27 ′ N and longitudes 97 o 22 ′ E to 105 o 37 ′ E. The total area is 513,115 square kilometers or around 200,000 square miles. The boundaries of Thailand with adjacent areas are:

- North: Myanmar and Laos.
- East: Laos, Cambodia and the Gulf of Thailand.
- South: Malaysia.
- West: Myanmar and the Andaman Sea.

From the meteorological point of view the climate of Thailand may be divided into three seasons as follows:

• *Rainy or southwest monsoon season* (mid-May to mid-October). The southwest monsoon prevails over Thailand and abundant rain occurs over the country. The wettest period of the year is August to September. The exception is found in the Southern Thailand East Coast where abundant rain remains until the end of the year that is the beginning period of the northeast monsoon and November is the wettest month.

• *Winter or northeast monsoon season* (mid-October to mid-February). This is the mild period of the year with quite cold in December and January in upper Thailand but there is a great amount of rainfall in Southern Thailand East Coast, especially during October to November.

• *Summer or pre-monsoon season*, mid-February to mid-May. This is the transitional period from the northeast to southwest monsoons. The weather becomes warmer, especially in upper Thailand. April is the hottest month.

Figure 1 Thailand boundary

B. Data collection

Multi-functional Transport Satellites (for example see in Figure 2) is a series of geostationary weather satellites operated by the Japan Meteorological Agency (JMA) [15]. MTSAT carries an aeronautical mission to assist air navigation, plus a meteorological mission to provide imagery over the Asia-Pacific region. The meteorological mission includes an image giving nominal hourly full Earth disk images in five spectral bands (one visible, four infrared). The satellites also have the capability to relay weather data from remote Automatic Weather Stations. The image wavebands and response functions for MTSAT-2.

•Visible (VIS):0.55 - 0.80 µm, Silicon (Si) photovoltaic detector
•Infrared (IR1): 10.3 - 11.3 µm, Mercury Cadmium Telluride (HgCdTe) photoconductive detector
•Infrared (IR2): 11.5 - 12.5 µm, Mercury Cadmium Telluride (HgCdTe) photoconductive detector
•Water Vapour (IR3): 6.5 - 7.0 µm, Mercury Cadmium Telluride (HgCdTe) photoconductive detector
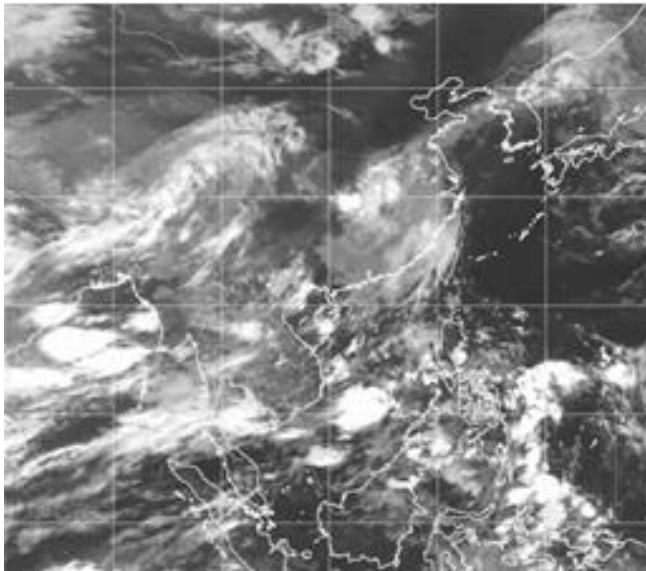•Near Infrared (IR4): 3.5 - 4.0 µm, Indium Antimonide (InSb) photovoltaic detector

Figure 2. The sample of MTSAT-2 data

C. Rainfall data

Monthly and annual rainfall data were collected from Thai Meteorological Department (TMD) in the year Thailand 2011. These data were created by the interpolation of rainfall records acquired from 115 weather stations (see in Table 1) [16] covering Thailand using the Kriging interpolation [17].

Table 1. Raining classes in 2011

Raining Classes	Area in s.q.km	Percentage
[1] 0-900	369.60	0.08
[2] 900-1,000	1,491.60	0.31
[3] 1,000-1,100	4,738.80	0.99
[4] 1,100-1,200	14,946.80	3.13
[5] 1,200-1,300	47,203.20	9.90
[6] 1,300-1,400	115,742.00	24.27
[7] 1,400-1,500	105,124.80	22.04
[8] 1,500-1,600	59,078.80	12.39
[9] 1,600 - 1,700	25,066.80	5.26
[10] > 1,700	103,166.80	21.63

III. METHODOLOGY

A. Develop algorithm for precipitation assessment

The author has been developed a new Matlab programming for subset boundary of Thailand from the whole images. The four specific coordinates represented to Thai boundary were chosen and listed as position A, B, C and D, where their respective coordinates are: A (96°E, 22°N); B (107°E, 22°N); C (96°E, 5°S) and D (107°E, 5°S).

B. Radiance to brightness temperature

The Planck Function [18] is used frequently to compute the radiance emitted from objects that radiate like a perfect "Black Body". Its derivation is one of the triumphs of 20th Century physics. The inverse of the Planck Function is used to find the "brightness temperature" of an object whose emitted radiance has been measured. The precise formula for the Planck function depends on whether the radiance is reckoned on a "per unit wavelength" basis or a "per unit frequency" basis. In the former case, the formula is equation 1.

$$B_i(T_b) = \frac{2hc^2 v_i^3}{\exp\left[hcv_i / k\left(a_{1i} + a_{2i}T_b\right)\right]-1} \tag{1}$$

Where; B_i is the Planck function (or observed radiance) of sensor's channel i; T_b is the brightness temperature (TBB); v_i is central wave number of channel i; a_{1i}, a_{2i} are band correction coefficients of channel i; h, k are Planck and Boltzmann constants respectively; c is the speed of light in vacuum. The values of the constants a_1 and a_2 for each MTSAT-2 data are given in Table 2 [19]. In this context, TBB is the equivalent temperature at the surface of objects under observation (e.g., clouds) from which the measured radiance was first released.

C. A priori knowledge–based threshold

The bi-spectral method [20], [21] was used to classify the cloud types. Based on the bi-spectral method the author used a TBB of 253 Kelvin (K) for the cloud threshold of deep convection, and brightness temperature difference (BTD) between the bi-spectral method (BTD=TBB$_{11}$- TBB$_{12}$) of 1.0 K for the cirrus and cumulonimbus type cloud classifications. A deep convection is defined as a cloud area colder than 253K TBB. Cumulonimbus type cloud area is defined as having a BTD below 1.0 K within the deep convection. The Cirrus type cloud area is defined as having a BTD greater than 1.0 K.

Table 2. The values constants a_1 and a_2 for MTSAT-2

Channel	Wave number	Band correction coefficients	
	v (cm^{-1})	a_1	a_2

IR1 (10.8 μm)	926.4627	0.3597851	0.9987568
IR2 (12.0 μm)	835.6672	0.2195110	0.9991676
IR3 (6.80 μm)	1476.6898	0.3645235	0.9991492
IR4 (3.80 μm)	2684.1181	2.4635230	0.9967825

IV. RESULT

In this work was succeeded by using MATLAB programming for subset boundary of Thailand from the whole images (see in Figure 3). The four specific coordinates represented to Thai boundary were chosen and listed as position A, B, C and D, where their respective coordinates are: A (96°E, 22°N); B (107°E, 22°N); C (96°E, 5°S) and D (107°E, 5°S). The subset images now contain 220x340 pixels. The Japan Meteorological Agency (JMA) posts MTSAT-2 data when the satellite data are completely received at the ground reception system. It usually takes an hour to process the satellite data, generate the data, and upload it to the MTSAT website. The user can download it from http://www.jma.go.jp/jma/jma-eng/satellite/index.html. There is much satellite data, and remote sensing commercial software is currently available for this research, The IR on MTSAT-2 satellite data requires converting to temperature using the look-up table provided by the JMA [15].
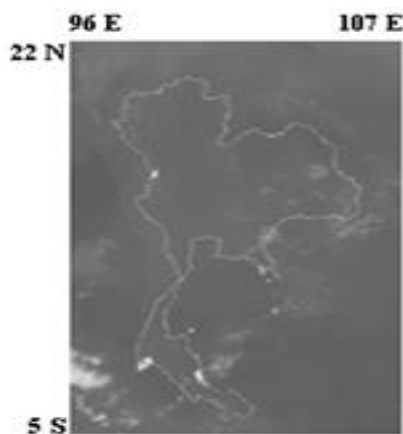

Figure 3 Subset boundary of Thailand

The bi-spectral (BTD=TBB_{11}-TBB_{12}) method was used to represent cloud distribution patterns; their data taken on 07 February 2011 were used for the analysis. Mainly potential warm clouds at 263K-283K were seen in the afternoon, but some can last all night long. For example amounts of cloud cover at each temperature are shown in Figure 4.
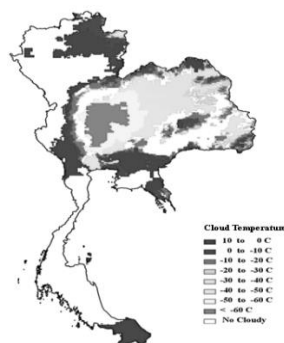

Figure 4. Cloud cover at each temperature

V. CONCLUSIONS

This article presents the development of algorithm for assessment of cloud properties in the atmosphere using satellite data. The author has been developed a new Matlab programming for subset boundary of Thailand from the whole images. The four specific coordinates represented to Thai boundary were chosen and listed as position A, B, C and D, where their respective coordinates are: A (96°E, 22°N); B (107°E, 22°N); C (96°E, 5°S) and D (107°E, 5°S). From satellite data, convert radiance to brightness temperature using Planck function theory and bi-spectral method was used to classify the cloud types.

ACKNOWLEDGEMENT

REFERENCES

1. G M.P. Jensen, A.M. Vogelmann, W.D. Collins, G.J. Zhang, E.P. Luke, Investigation of regional and seasonal variations in marine boundary layer cloud properties from MODIS observations. *Journal of Climate*, 21, 2008, pp. 4955–4973.
2. P. A. Richard. Combining satellite data and models to estimate cloud radiative effect at the surface and in the atmosphere. Department of Meteorology/National Centre for Atmospheric Science, School of Physical and Mathematical Sciences, University of Reading, Reading, Berks RG6 6AL, UK, 2011.
3. B.J. Sohn, Cloud-induced infrared radiative heating and its implications for the large-scale tropical circulation. *Journal of the Atmospheric Sciences*, 56, 1999, pp. 2657–2672.
4. W. Su, A. Bodas-Salcedo, K.M. Xu, T.P. Charlock, Comparison of the tropical radiative flux and cloud radiative effect profiles in a climate model with Clouds and the Earth's Radiant Energy System (CERES) data. *Journal of Geophysical Research*, 115, 2010.
5. Y. J. Kaufman, A. Smirnov, B. N. Holben, and O. Dubovik, Baseline maritime aerosol: Methodology to derive the optical thickness and scattering properties, *Geophys. Res. Lett*., 28, 2001, pp. 3251–3254.
6. D. Kim, and V. Ramanathan, Solar radiation budget and radiative forcing due to aerosols and clouds, J. Geophys.Res., 113, 2008, D02203, doi: 10.1029/2007J D0 08434.
7. F. J. Turk, P. Arkin, E.E. Ebert, and M. Sapiano, Evaluating high-resolution precipitation products, B. *Am. Meteorol. Soc*., 89, 2008, pp. 1911–1916.
8. I. M. Lensky, and D. Rosenfeld, Clouds-Aerosols-Precipitation Satellite Analysis Tool (CAPSAT), *Atmos. Chem. Phys*., 8, 2008, pp. 6739-6753.
9. M. Grecu, and W. S. Olson, Precipitating snow retrievals from combined airborne cloud radar and millimeter-wave radiometer observations, *J. Appl. Meteorol. Climatol*. 47, 2008, pp. 1634–1650.
10. D. Capacci, and F. Porcu, Evaluation of a satellite multispectral VIS–IR daytime statistical rainrate classifier and comparison with passive microwave rainfall estimates, *J. Appl. Meteorol. Climatol*, 48, 2009, pp. 284–300.
11. A. D. Fraser, Massom, R. A. and K. J. Michael, Generation of high-resolution East Antarctic land fast sea-ice maps from cloud-free MODIS satellite composite imagery, *Remote Sensing of Environment*, 114, 2010, pp. 2888-2896.
12. R. Frey, S. A. Ackerman, Y. Liu, K. I. Strabala, H. Zhang, J. Key, and X. Wang. Cloud detection with MODIS: Part I. Improvements in the MODIS Cloud Mask for Collection 5, *J. Atmos. Oceanic Technol*., 25, 2008, pp. 1057– 1072.
13. B. Tang, and Z.L. Li, Estimation of instantaneous net surface long wave radiation from MODIS cloud-free data. *Remote Sensing of Environment*, 112, 2008, pp. 3482-3492
14. Z. Yao, Z. Han, Z. Zhao, L. Lin, and X. Fan, Synergetic use of POLDER and MODIS for multilayered cloud identification. *Remote Sensing of Environment*, 114, 2010, pp. 1910-1923.

15. Monitoring the earth from the MTSAT, 2013, online available at http://mscweb.kishou.go.jp/index.htm
16. Rainfall data, 2011, Thai Meteorological Department, online available at http://www.tmd.go.th/en/
17. P.A. Burrough, & R.A. McDonnell, 1998, Principles of Geographical Information Systems. Oxford: Oxford University Press.
18. R.B. Smith, 2005, Computing the Planck Function, Yale University, online available at http://www.yale.edu/ceo/ Documentation/ ComputingThePlanckFunction.pdf
19. Teerawong Laosuwan, Singthong Pattanasethanon, and Worawat Sa-ngiamvibool, Automated Cloud Detection of Satellite Imagery Using Spatial Modeler Language and ERDAS Macro Language, *IETE Technical Review*, 30 (3), pp 183-190, 2013.
20. T. Inoue, Features of clouds over the tropical pacific during northern hemispheric winter derived from split window measurements. *J. Meteor. Soc. Japan*, 67, 1989, pp. 621-637.
21. T. Inoue, M. Satoh, Y. Hagihara, H. Miura, and J. Schmetz, Comparison of high-level clouds represented in a global cloud system–resolving model with CALIPSO/CloudSat and geostationary satellite observations, *J. Geophys. Res.*, 115, 2010, D00H22, doi: 10.1029/2009JD012371, [printed 116(D4), 2011].

132